Ultraviolet-infrared femtosecond laser-induced damage in fused silica and CaF_2 crystals

T. Q. Jia
The Institute for Solid State Physics, The University of Tokyo, 5-1-5 Kashiwanoha, Kashiwa, Chiba 277-8581, Japan and State Key Laboratory of High Field Laser Physics, Shanghai Institute of Optics and Fine Mechanics, Chinese Academy of Sciences, P.O. Box 800-211, Shanghai, China

H. X. Chen, M. Huang, and F. L. Zhao
State Key Laboratory of Optoelectronic Materials and Technologies, Zhongshan University, Guangzhou, 510275, Peoples Republic of China

X. X. Li, S. Z. Xu, H. Y. Sun, D. H. Feng, C. B. Li, X. F. Wang, R. X. Li, and Z. Z. Xu
State Key Laboratory of High Field Laser Physics, Shanghai Institute of Optics and Fine Mechanics, Chinese Academy of Sciences, P.O. Box 800-211, Shanghai, China

X. K. He and H. Kuroda
The Institute for Solid State Physics, The University of Tokyo, 5-1-5 Kashiwanoha, Kashiwa, Chiba 277-8581, Japan
(Received 11 May 2005; revised manuscript received 12 October 2005; published 16 February 2006)

The damage in fused silica and CaF_2 crystals induced by wavelength tunable femtosecond lasers is studied. The threshold fluence is observed to increase rapidly with laser wavelength λ in the region of 250–800 nm, while it is nearly a constant for $800<\lambda<2000$ nm. The ultrafast electronic excitation is also studied by a pump and probe method. The reflectivity increases rapidly in the latter half of pump pulse, which supports that impact ionization plays an important role in the generation of conduction band electrons (CBEs). We study the CBEs absorption via subconduction-band (sub-CB) transition, and develop a coupled avalanche model. Our results indicate that the CBEs absorption via sub-CB transition plays an important role in the damage in dielectrics irradiated by the visible and near ultraviolet femtosecond lasers. Our theory explains well the experiments.

DOI: 10.1103/PhysRevB.73.054105 PACS number(s): 61.80.Ba, 78.47.+p, 79.20.Ds

I. INTRODUCTION

Femtosecond (fs) laser-induced damage in dielectrics and its application in the field of microfabrication have been studied intensively.[1–14] During the last decade, much attention was paid to near infrared (NIR) fs lasers. Recently, ultrashort excimer lasers progressed rapidly, and it was widely applied to study the ablation and microfabrications in solid materials.[15–17] Reference 17 reported the dependence of ablation rate on the 248 nm laser pulse duration (200 fs–50 ps), and found that it was nearly a constant as pulse duration less than 20 ps. References 1, 9, and 18 studied the ablation and microfabrication using the visible fs lasers obtained by frequency doubling via nonlinear crystals. Soft x rays were also reported recently to be used in the ablation and microfabrication in dielectrics and polymers.[19–21]

Recently, wavelength tunable laser-induced damage in solid materials attracted much attention. Reference 22 reported the optical breakdown in transparent dielectrics as a function of laser wavelengths ($\lambda=4.7–7.8$ μm), and found that the threshold fluences decreased from 6 to 2 J/cm^2 as laser wavelengths increased from 4.7 to 7.8 μm, here the pulse duration was 1 ps. References 23 and 24 studied the wavelength dependence (1200–193 nm) of nanosecond laser-induced damage in transparent materials. However, the damage in dielectrics induced by wavelength tunable fs lasers has not been reported.

Many theoretical investigations have been concentrated on the damage in dielectrics induced by the NIR fs lasers.[25–28] It was proposed that the valence band electrons were excited to the conduction band (CB) via photoionization (PI),[1,2] which included multiphoton ionization and tunneling ionization. The conduction band electrons (CBEs) absorbed laser energy via inverse bremsstrahlung. When its kinetic energy was larger than the band gap, it impacted with another valence band electron, and excited the latter to CB. This impact ionization (II) would induce CBEs numerical density to increase exponentially. Obviously, the process for CBEs absorbing laser energy played a very important role in II and laser energy deposition in samples. The absorption rates W were calculated by classical method or quantum perturbation theory.[29,30] The rates increased nonlinearly with laser wavelengths $\lambda: W\propto\lambda^2-\lambda^3$. Several theoretical models have been developed on the basis of the above fundamental concept of the avalanche theory, and explained the experimental phenomena such as the damage threshold, ablation rate, filamentation, and electronic ultrafast dynamics.[5,9,28] However, the damage mechanisms in dielectrics induced by the visible and near ultraviolet (NUV) fs lasers were far from fully understood.[15,16]

In this paper, we study the optical breakdown in fused silica and CaF_2 crystals induced by wavelength tunable fs lasers (2000–260 nm). The threshold fluences are observed to be nearly a constant in the NIR region, and decrease rapidly with laser wavelength in the visible and NUV regions.

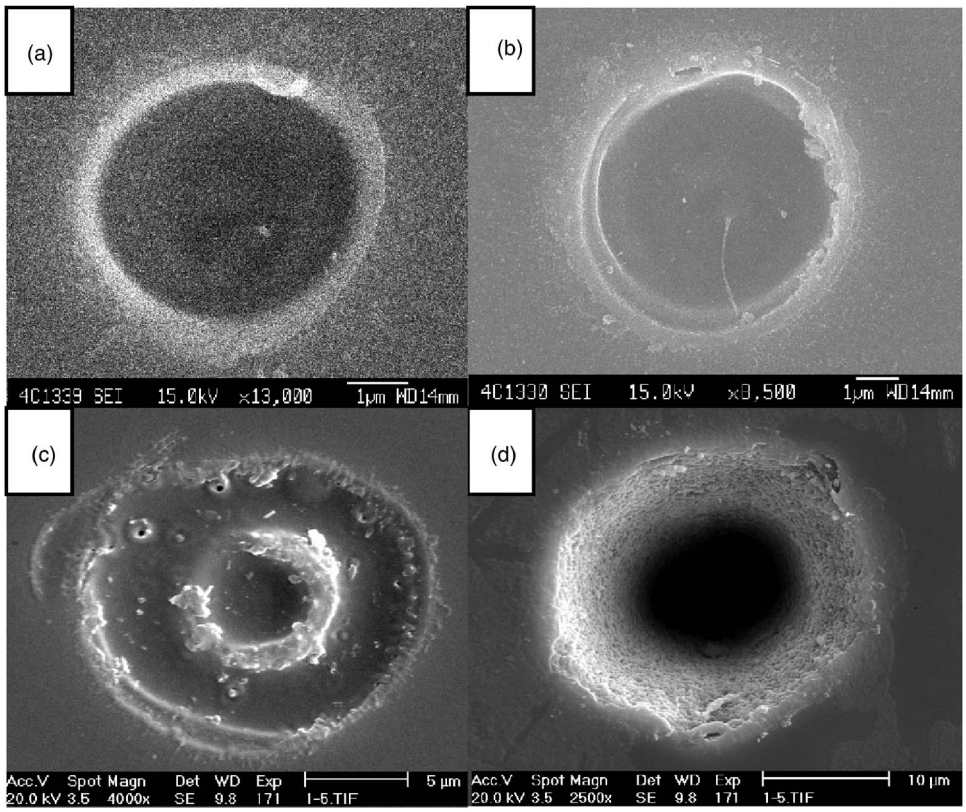

FIG. 1. SEM images of the ablation craters induced by fs lasers at wavelengths of 1710 nm, 11 μJ (a), 1200 nm, 17 μJ (b), 400 nm, 25 μJ (c) and (d). (a)–(c) are induced by three pulses, and (d) by 100 pulses.

We study the time-resolved electronic excitation using a pump and probe system, and find that the reflectivity increases rapidly in the latter half of the pump pulse duration. This supports that II plays an important role in CBEs production. We study the CBEs absorption via inverse bremsstrahlung and via the direct transition between different sub-conduction-band (sub-CB), and explain well the damage threshold and ultrafast electronic dynamics.

II. EXPERIMENTAL SETUP AND RESULTS

800 nm, 150 fs laser pulse with energy of 0.7 mJ is delivered from a Ti:sapphire laser system (Spectra Physics).[31] It was used to stimulate an optical parametric amplifier, and generated lasers tunable from 500 to 2200 nm with pulse energy between 11 and 48 μJ. The tunable pulses went through a Glan polarizer, then focused perpendicularly on the front surface of sample with a microscopic lens [numerical aperature (NA)=0.25]. In order to obtain NUV laser pulses, the 800 nm laser frequency was doubled through a BBO crystal of 0.5 mm thick, then split into two beams at wavelengths of 800 and 400 nm, respectively. The 800 nm laser beam went through a delay line and was collinear with the 400 nm one. The laser pulse at 267 nm could be obtained by a BBO crystal of sum frequency. The 267 and 400 nm lasers were focused on the sample surface with a silica lens. The samples were mounted on a *XYZ*-translation stage, and moved after each site irradiated by three pulses.

The experiments of ultrafast electronic excitation were conducted on another Ti:sapphire laser system (Spectra Physics). The pulse duration was 50 fs at wavelength of 800 nm. The laser frequency was, similar to the above setup, doubled through a BBO crystal, then split into a pump pulse (800 nm) and a probe pulse (400 nm). The pump pulse duration τ was stretched from 50 to 800 fs through ZF6 glass plate, then it went through a delay line. The pulse duration was monitored with an autocorrelater. The pump and the probe laser beams were focused by two silica lenses with 400 mm focal length, respectively. Then, they were collinear and confocal on the front surface at an incident angle of 10°. Their focus diameters were measured to be 53 μm with a knife edge method. The sample surface was monitored with a microscope and a charge coupled device (CCD) camera, which ensured the confocal error less than 10 μm. The zero point was determined by measuring the pulse energy of the sum frequency (267 nm). The ratio of the pump and the probe pulse energy was larger than 50:1, their wavelengths were also different. Therefore, the interference between the two pulses was avoided when they reached simultaneously at the sample surface. The probe pulse went through a prism and was separated from the pump one, its reflectivity was measured with an energy meter (J3S-10, EPM1000, Molectron Detector Inc).

The samples studied here are fused silica and CaF_2 crystals. They are about 1 mm thick, and the two surfaces are both polished, with roughness less than 15 nm.

The ablation craters are measured with optical microscope and scanning electronic microscope (SEM). The SEM images are shown in Fig. 1. The laser wavelengths change from the NUV to NIR region, but the ablation craters are similar, namely, with clear edge and no evidence of heat diffusion.[32–35] When laser fluence is much higher than the threshold, there will be a heavy ablation region in the center

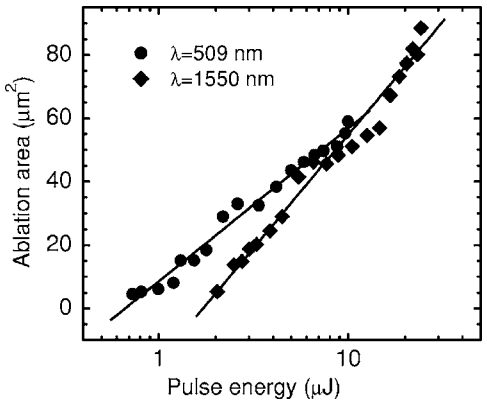

FIG. 2. The ablation area of the craters in fused silica as a function of laser pulse energy.

of laser focus [Fig. 1(c)].[36,37] Figure 1(d) shows the regular hole ablated by 100 pulses at wavelength of 400 nm, and it is similar to the hole induced by 5 fs laser pulses at wavelength of 800 nm.[8]

The damage threshold was determined by the criterion of visible permanent modification or plasma emission.[1,2] We measure the ablation craters, and find that the areas S increases logarithmically with laser fluences F, $S \propto \ln(F/F_{th})$.[28,38] The solid circles and diamonds in Fig. 2 show the results for fused silica irradiated by lasers at 509 and 1550 nm, respectively. By extrapolating the regression line (shown as the solid line) to $S=0$, we can obtain the threshold fluences F_{th}.

Reference 23 studied the wavelength dependence of ns laser-induced damage in deuterated potassium dihydrogen phosphate crystals, and observed two steps in the dependence of $F_{th} \sim \lambda$ when the photon energy $\hbar\omega$ satisfied the formula: $K\hbar\omega = E_g$, here K was 3 and 4 and E_g was the band gap. This wavelength dependence suggested that the damage was initiated from multiphoton absorption. The threshold fluences of fused silica and CaF_2 crystals are presented in Fig. 3. It is about 0.9 J/cm^2 in fused silica as laser wavelengths $\lambda = 267$ nm, and increases rapidly to 2.3 J/cm^2 as $\lambda = 800$ nm. The threshold fluences for the visible lasers correspond well to the results reported previously,[2,9] and there is no large step in the dependence $F_{th} \sim \lambda$. We think besides PI, II may also play an important role in the damage in dielectrics induced by fs lasers. The threshold fluences become nearly a constant as $800 < \lambda < 2000$ nm. The spectroscopy of the fundamental 150 fs, 800 nm laser is not very wide (790–810 nm), the pulse duration is only slightly changed through the optical parametric amplifier. Hence, we think the tunable pulse durations also equal 150 fs. As $\lambda > 4.7$ μm, Ref. 22 reported that the threshold fluences began to decrease with the increase of laser wavelengths, which was explained by the avalanche model.

Many studies were focused on the ultrafast electronic dynamics in dielectrics.[39–44] However, the durations of the pump and the probe pulse were equal; only the relaxation processes such as electron-phonon interaction and the formation of self-trapped excitons were studied intensively. The time-resolved excitation processes could not be investigated. Therefore, significant controversies remained about the electronic excitation in dielectrics irradiated by fs lasers. Reference 2 proposed that II played the dominant role in CBEs production, and explained the dependence of threshold fluences F_{th} on the pulse duration. However, Refs. 10, 11, and 26 suggested that the time required for II to take place was long, and it did not play an important role in CBEs production.

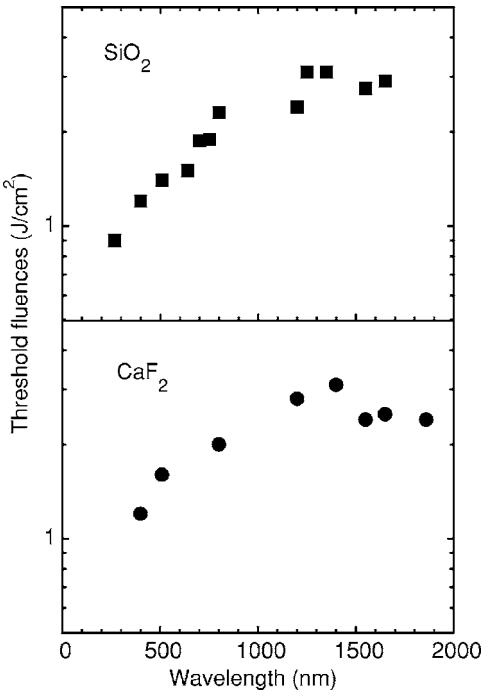

FIG. 3. Threshold fluences vs laser wavelengths.

We stretch the pump pulse duration to 600 fs, and keep the probe pulse less than 60 fs, so that we can investigate the ultrafast time-resolved electronic excitation. The results are shown in Fig. 4. When the pump pulse energy ($E_p = 160$ μJ) is much higher than the threshold value (90 μJ),[9,28] the valence band electrons are quickly excited up to CB, and cause the reflectivity R to increase rapidly. This is not caused by the lattice melting, because ultrafast melting usually takes place after the peak of pump pulse.[45–47] As E_p decreases to 120 μJ, R begins to increase at the peak of pump pulse, and enhances greatly during the latter half. The results can be explained well by avalanche theory[1,2]: the seed CBEs are produced quickly via PI at the peak of pump pulse, which will trigger II in the latter half, and cause CBEs density n_e to increase exponentially. Here, the zero point is measured for six times, its error is less than ±10 fs.

III. THEORY

The experimental results (see Fig. 4) about the ultrafast dynamics in fused silica and CaF_2 crystals indicate that II plays an important role in CBEs production. The II rate depends mainly on the rate that CBEs absorb energy from the laser field. In our theory, we study the absorption rate, and propose that the absorption via the direct transition between different sub-CB is very important for the visible and NUV

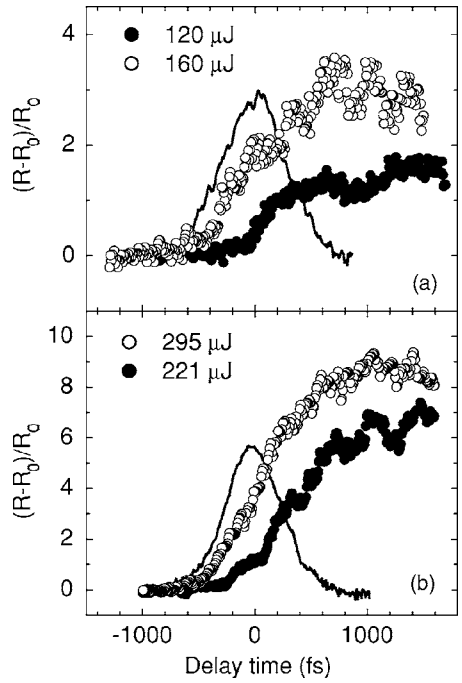

FIG. 4. The ultrafast evolution of the reflectivity R in fused silica (a) and CaF_2 crystals (b), here R_0 is the initial reflectivity. The solid curves present the correlation function of the pump and probe pulses.

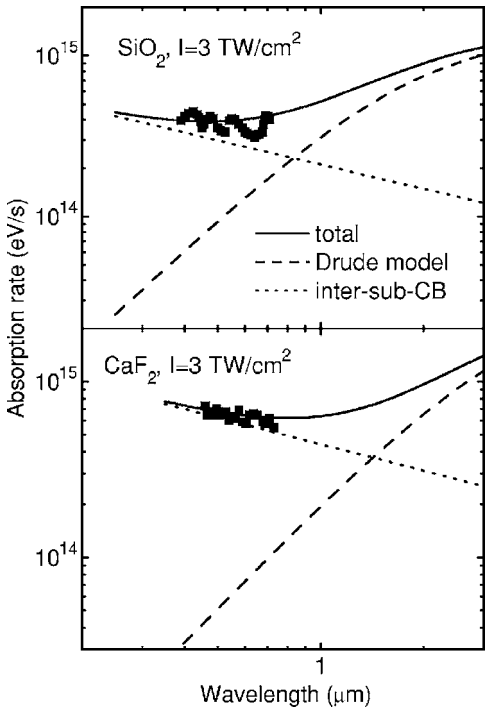

FIG. 5. The CBEs absorption rate vs laser wavelengths.

lasers. Then, we calculate the II rate and PI rate by the flux-doubling model and the Keldysh theory, respectively. We solve numerically the coupled equations of CBEs density $n_e(t)$ and the effective dielectric function $\varepsilon^*(\hbar\omega, n_e)$, and obtain the wavelength dependence of threshold fluences.

A. CBEs absorption rate

Electrons move in the laser electric field, and can absorb laser energy continuously. The absorption rate W_D is described by Drude model[2]

$$W_D = \frac{1}{3}\sigma E_l^2,$$

$$\sigma = \frac{e^2\tau_D}{m^*[1+\omega^2\tau_D^2]}, \tag{1}$$

here σ is the conductivity per electron, E_l is the amplitude of laser electric field, and CBEs effective mass m^* is taken as that of a free electron. τ_D is the CBEs scattering time with lattice; it is calculated and measured to be of the order of 1 fs in fused silica.[29,48] The absorption rate calculated with Eq. (1) is shown as the dashed curve in Fig. 5, which increases rapidly with laser wavelengths. CBEs decaying time in CaF_2 is measured to be about 700 fs, and it is longer than that in fused silica.[39,49–51] Here we take the scattering time τ_D is 2.0 fs (see Table I).The factor 1/3 is enclosed for the random direction of CBEs momentum after scattering with lattice.[2,52,53]

The Drude model explained the optical properties in the infrared region in metals and semiconductors. However, it deviated greatly from the measurements in the visible and NUV regions.[54–59] References 60 and 61 have studied the transient absorption spectroscopy of electron-hole pairs in fused silica and CaF_2 crystals with pump and probe method. The 800 nm femtosecond laser beam was split into two beams. One beam is tripled via BBO crystals, and was used as the pump pulse to generate electron-hole pairs in transparent dielectrics. The other beam is focused into water cell to produce white-light pulse. The time-resolved optical absorption spectroscopy was observed to be very wide and uniform in the visible region. The experimental results are shown as the solid squares in Fig. 5, which also deviates greatly from the Drude model.

It was proposed that for the visible light, the absorption via the transition between sub-CB played an important role in semiconductors and metals.[54–58] The absorption rate W_{sub} via direct sub-CB transition is

$$W_{sub} = f_{sub}\frac{e^2(\hbar\omega-\hbar\omega_0)^{3/2}}{m^*\hbar\omega}E_l^2, \tag{2}$$

here $\hbar\omega_0$ is the band gap between sub-CB. The electronic band structures in SiO_2 and CaF_2 have been calculated using

TABLE I. Modeling parameters for fused silica and CaF_2

Parameters	Fused silica	CaF_2
E_g (eV)	8.0	10.0
τ_D (fs)	1.0	2.0
f_{sub} (10^{-7} s/J$^{1/2}$)	1.8	3.1
N_0 (10^{22}/cm^3)	2.2	2.45
E_{dep} (kJ/cm^3)	54	49

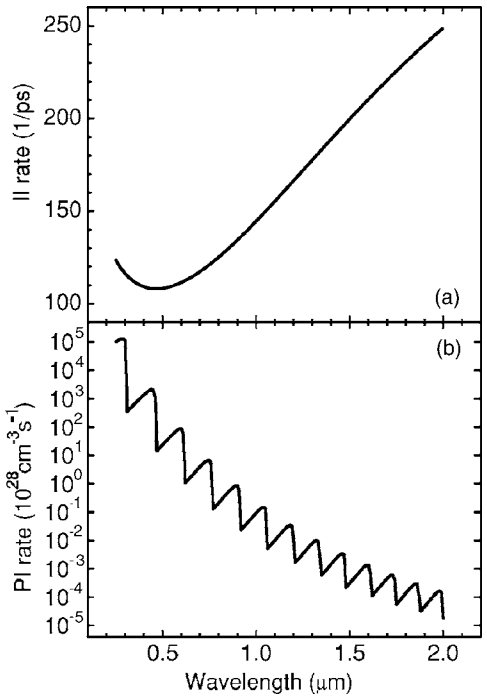

FIG. 6. The wavelength dependences of the II rate (a) and the PI rate (b) in fused silica irradiated by lasers for intensity $I=3$ TW/cm^2.

ab initio method and self-consistent pseudopotentials method.[62,63] The results indicated that there are many sub-CB in the range of 0–10 eV above the CB bottom. Therefore, we propose the CBEs absorption via sub-CB transition plays an important role in the visible and NUV regions. Exact calculation of the absorption rate requires the electronic band structures, state densities, and electron dispersion, which is far beyond the present papers.[64] We estimate the factor f_{sub} by simulating the measured absorption spectroscopy in the visible and NUV regions. f_{sub} and other parameters are shown in Table I. If W_{sub} is considered, the theory explains well the experimental measurements (see Fig. 5), here $\hbar\omega_0$ is taken as zero. The absorption rate via inverse bremsstrahlung is larger than that via sub-CB transition in the NIR region, but for the visible and NUV lasers, the CBE absorption via sub-CB transition is very important.

B. Coupled avalanche model

The II rate is calculated using the flux-doubling model, the results are shown in Fig. 6(a), here the critical energy for impact ionization is taken as $1.5\times E_g$.[11] The factor 1.5 is introduced for the conservation of CBEs momentum. Figure 6(b) shows the PI rate calculated by Keldysh theory.[65]

The evolution equation of CBEs numerical density n_e can be written as

$$\partial n_e/\partial t = (R_{PI} + R_{II} n_e)(1 - n_e/N_0), \qquad (3)$$

R_{II} and R_{PI} are the II rate and PI rate, respectively. The factor $1-n_e/N_0$ is introduced for the consideration of the exhaust of valence band electrons, the initial density $N_0=2.2\times10^{22}$ cm^{-3} in fused silica.[66]

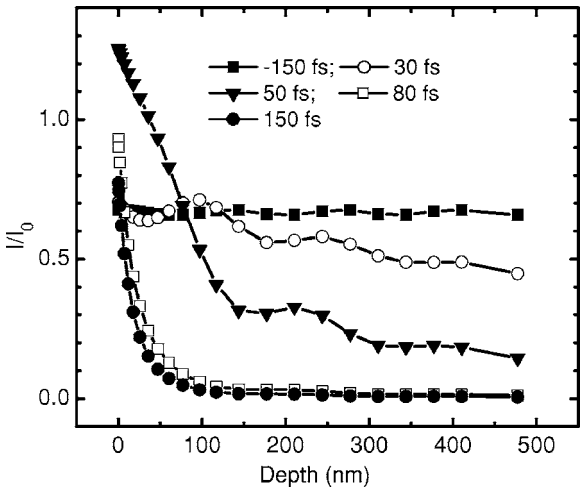

FIG. 7. The evolution of the distribution of laser intensity in fused silica, the 0 depth is at the sample surface.

The ultrafast evolution of reflectivity of the probe pulse (shown in Fig. 4) indicates clearly that the optical characteristics in the sample change greatly during the pump laser irradiation, which will inversely influence the transmission and the distribution of the pump pulse itself. Therefore, we develop a coupled dynamic model. It considers not only the processes in a sample excited by pump laser pulse, but also studies simultaneously the inverse influences of this excitation on the pump lasers.

The effective dielectric function ε^* changes with n_e, the dependence can be written as

$$\varepsilon^*(\hbar\omega) = 1 + (\varepsilon(\hbar\omega) - 1)\frac{N_0 - n_e}{N_0} - f\frac{e^2 n_e}{\varepsilon_0 m^* m_e \omega^2}, \qquad (4)$$

here $\varepsilon(\hbar\omega)$ is dielectric function of the unexcited material.[67] Because the absorption via sub-CB transition is considered, the imaginary part of the effective dielectric function ε^* will increase correspondingly. The factor f is taken as $1/3[1/(1+i/\omega\tau_D)]+i f_{sub}[(\hbar\omega-\hbar\omega_0)^{3/2}/\hbar\omega]$. In our numerical calculation, the change of ε^* mainly influences the distribution of laser fluence. It begins to vary greatly only when CBEs density is higher than 10^{21} cm^{-3}.

In order to calculate the spatial distribution of laser intensity I/I_0, we treat the bulk sample as a stack of 24 thin layers.[27] Here I_0 is the laser intensity in air, it is Gaussian pulse in temporal and spatial distribution: $I_0=I_{\max}\times\exp[-4\ln 2(t^2/\tau^2)]\exp(-r^2/w_0^2)$. The thickness of each layer is (0.01, 0.02, 0.03, 0.05, 0.07, 0.09, 0.12, 0.15, 0.17, 0.2, 0.25, 0.3, 0.3, 0.4, 0.5, 0.5, 0.5, 0.5, 0.5, 0.5, 0.5, 0.5, 1.0, and 1.74) $\times\lambda/4n$. First, we calculate the distribution of laser intensity with transmitting matrix method, then resolve Eq. (3) numerically to study n_e evolution, and further calculate ε^* by Eq. (4). Hereafter, we recalculate the intensity distribution. This recycle is repeated each 2 fs during $-\tau$ to $+\tau$, hence the coupled Eqs. (3) an (4) are resolved.

C. Results

Figures 7–9 show the distribution of laser intensity, di-

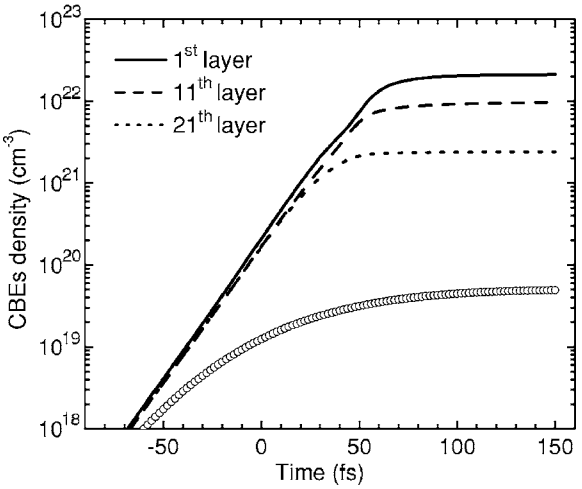

FIG. 8. The evolution of CBEs density in the first, the 11th, and the 21th layer in fused silica. The circles are the calculation results when CBEs absorption via sub-CB transition is not considered.

electric function, and CBEs density in fused silica irradiated by 400 nm, 1.6 J/cm^2, 150 fs lasers. The laser intensity in fused silica is about 70% of the value in air. CBEs are excited via PI and II; their density increases to 2×10^{21}/cm^3 at +30 fs (see Fig. 8). This will cause the refractive index n to decrease and the extinction coefficient k to increase, which will influence the distribution of laser intensity (see Figs. 7 and 9). When $t=+50$ fs, CBEs density will reach 10^{22}/cm^3, and the effective dielectric function ε^* and the reflectivity R will decrease to their minima (see Fig. 9). At this moment, 400 nm laser is a local transition mode, it can resonantly transmit through the sample.[68–70] The laser intensity is localized in the sample surface ($I=1.3I_0$, see Fig. 7). Hereafter, ε^* increases with CBEs density, while I/I_0 begins to decrease. It is shown clearly that the absorption via sub-CB transition plays an important role in CBEs production. If it is not considered, CBEs density at sample surface will decrease by more than three orders (see the circles in Fig. 8).

We calculate the integral $\int n_e W\,dt$, and obtain the evolution of laser energy density E_{dep} deposited in the sample. As

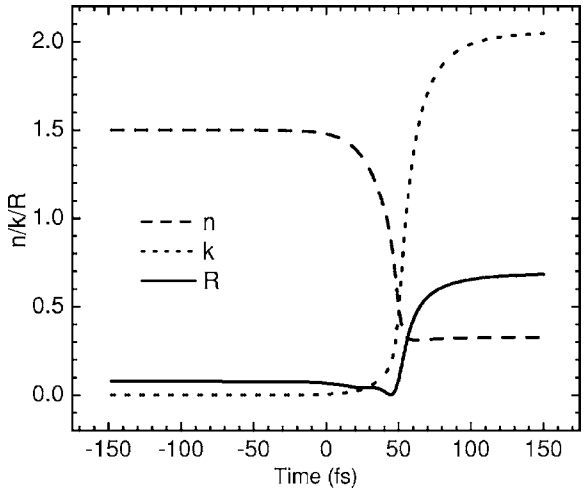

FIG. 9. The refractive index n, extinction coefficient k and reflectivity R in the first layer in fused silica.

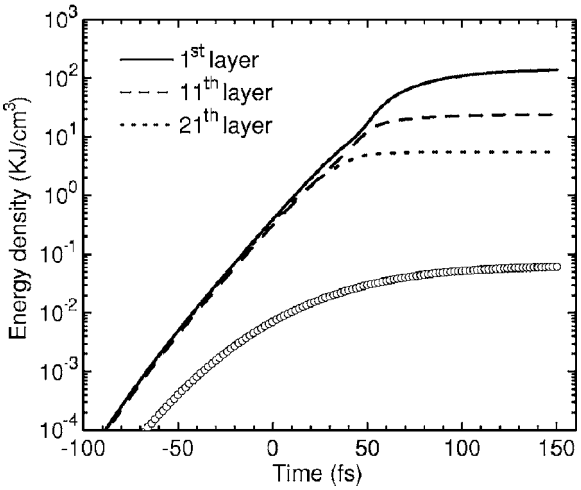

FIG. 10. The energy density deposited in the first, the 11th, and the 21th layer in fused silica.

shown in Fig. 10, E_{dep} in the sample surface will reach 100 kJ/cm^3 at the end of laser pulse. However, it is less than 0.1 kJ/cm^3 if the sub-CB transition is not included in CBEs absorption, which is shown as the circles in Fig. 10. We choose the damage criterion of fused silica as $E_{dep}=54$ kJ/cm^3, and obtain the wavelength dependence of $F_{th}\sim\lambda$. Here CBEs diffusion is also considered.[27,28] The theoretical results are shown as the solid curve in Fig. 11. The PI rate decreases while the II rate increases in the NIR region, hence, the threshold changes slightly. It is about 2.2 and 2.5 J/cm^2 in fused silica and CaF_2 crystal, respectively. For the visible and NUV lasers, CBEs absorption rate and the II rate increase slightly when the absorption via sub-CB transi-

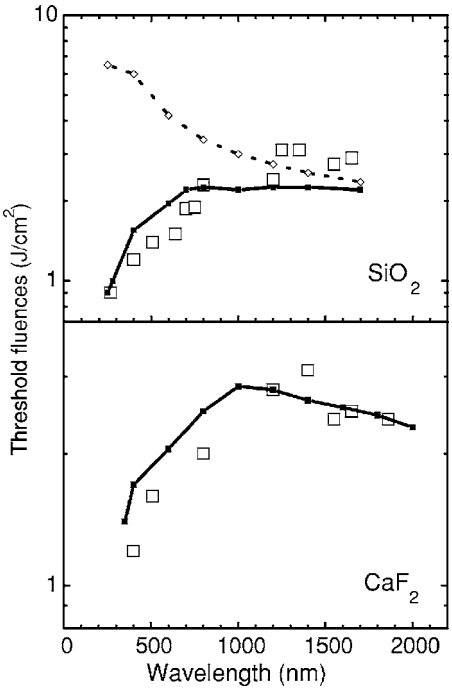

FIG. 11. The wavelength dependences of the threshold fluences in fused silica and CaF_2 crystals.

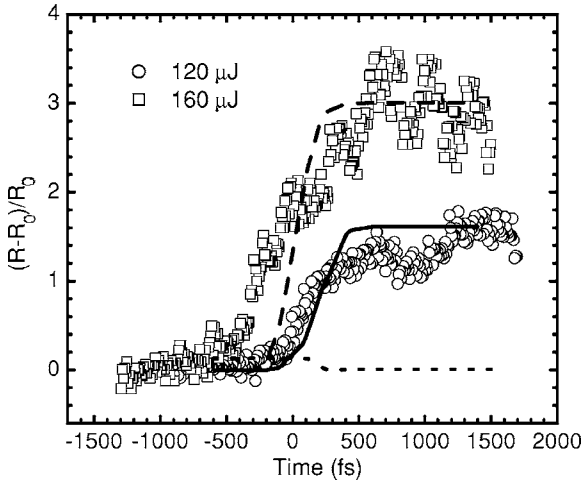

FIG. 12. The ultrafast evolution of the reflectivity of the 400 nm probe pulse.

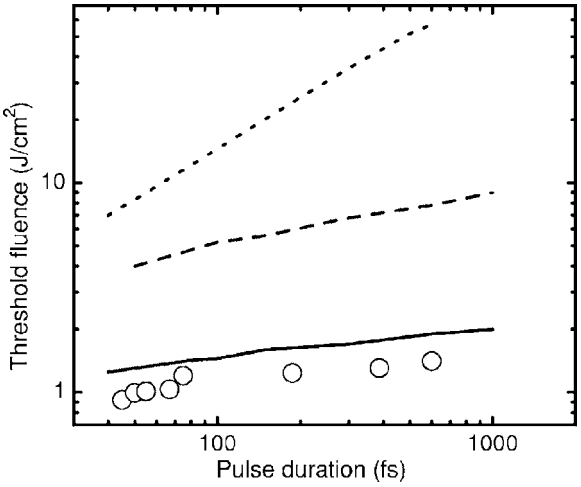

FIG. 13. The dependence of threshold fluences in fused silica on the 400 nm laser pulse durations. The circles are measurements from Ref. 9.

tion is considered. Meanwhile, the PI rate increases rapidly with the decrease of laser wavelength. Therefore, the threshold fluences decrease rapidly to 0.9 J/cm^2 as $\lambda=250$ nm, which agrees well with the experiments. If the absorption via sub-CB transition is not considered, the II rate will decrease rapidly. Therefore, the theoretical value will increase to 6.5 J/cm^2 as $\lambda=250$ nm (shown as the dotted curve), which is much higher than the measurements.

D. Discussion

The simulation result of the ultrafast dynamics in fused silica irradiated under 600 fs laser pulse is shown in Fig. 12. The solid and the dashed curves represent the calculated value for laser fluences $F=5.4$ and 7.2 J/cm^2, which corresponds to the pulse energy of 120 and 160 μJ, respectively. The spatial Gaussian distribution of laser beam is considered in our simulation. The coupled avalanche theory explains well the measurements, and supports the proposed mechanism that II plays an important role in CBEs production. If II is not considered, CBEs density produced via PI is only 10^{20}/cm^3, and the reflectivity will not change obviously. If the absorption via sub-CB transition is not considered, the imaginary part of the effective dielectric function for 400 nm lasers will decrease greatly, hence, the reflectivity will nearly decrease to zero, rather than increase by two times (shown as the dotted curve in Fig. 12). Our calculation indicates that if the laser fluences increase to 15 J/cm^2, the reflectivity will increase to more than 50%, which agrees well with recent experimental measurements.[3,71]

The dependence of threshold fluences in fused silica on the laser pulse duration is also calculated. The results are shown as the solid curve in Fig. 13. Our theory explains well the experimental measurements.[9] If the sub-CB transition is not considered, the threshold (the dashed curve) will be higher than the measurements by more than four times. If II is not considered, the threshold (the dotted curve) will be higher by ten times.

IV. CONCLUSION

We have studied wavelength tunable fs laser-induced damage in fused silica and CaF_2 crystals. The threshold fluences increase rapidly with laser wavelength in the region of 250–800 nm, while it is nearly a constant for $800<\lambda<2000$ nm. We have also studied the ultrafast electronic excitation using pump and probe method, and found that the reflectivity increases rapidly in the latter half of pump pulse. The results support the mechanisms that impact ionization plays an important role in CBEs production. We studied the CBEs absorption via sub-CB transition, and developed a coupled avalanche model. Our theory explains the threshold fluences and ultrafast dynamics. The results indicate that CBEs absorption via the sub-CB transition plays an important role in the damage in dielectrics irradiated by the visible and NUV fs lasers.

ACKNOWLEDGMENTS

The authors gratefully acknowledge Y. Liu, and H. Wang of Zhong-shan University, M. Baba, M. Suzuki, and F. Mitani of Tokyo University, and H. Lu and X. Ge of Shanghai Institute of Optics and Fine Mechanics for all of their help.

[1] D. Du, X. Liu, G. Korn, J. Squier, and G. Mourou, Appl. Phys. Lett. **64**, 3071 (1994); A. C. Tien, S. Backus, H. Kapteyn, M. Murnane, and G. Mourou, Phys. Rev. Lett. **82**, 3883 (1999).

[2] B. C. Stuart, M. D. Feit, A. M. Rubenchik, B. W. Shore, and M. D. Perry, Phys. Rev. Lett. **74**, 2248 (1995); B. C. Stuart, M. D. Feit, A. M. Rubenchik, B. W. Shore, and M. D. Perry, Phys. Rev. B **53**, 1749 (1996); B. C. Stuart, M. D. Feit, A. M. Rubenchik, B. W. Shore, and M. D. Perry, J. Appl. Phys. **85**,

6803 (1999).
[3] D. Von der Linde and H. Schüler, J. Opt. Soc. Am. B **13**, 216 (1996).
[4] R. Stoian, A. Rosenfeld, D. Ashkenasi, I. V. Hertel, N. M. Bulgakova, and E. E. B. Campbell, Phys. Rev. Lett. **88**, 097603 (2002); R. Stoian, M. Boyle, A. Thoss, A. Rosenfeld, G. Korn, I. V. Hertel, and E. E. B. Campbell, Phys. Rev. B **69**, 054102 (2004).
[5] Y. Shimotsuma, P. G. Kazansky, J. Qiu, and K. Hirao, Phys. Rev. Lett. **91**, 247405 (2003).
[6] J. Reif, F. Costache, S. Eckert, and M. Henyk, Appl. Phys. A: Mater. Sci. Process. **A79**, 1229 (2004).
[7] Y. Cheng, K. Sugioka, K. Midorikawa, M. Masuda, K. Toyoda, M. Kawachi, and K. Shihoyama, Opt. Lett. **28**, 1144 (2003).
[8] M. Lenzner, J. Kruger, S. Sartania, Z. Cheng, C. Spielmann, G. Mourou, W. Kautek, and F. Krausz, Phys. Rev. Lett. **80**, 4076 (1998).
[9] T. Q. Jia, Z. Z. Xu, X. X. Li, R. X. Li, B. Shuai, and F. L. Zhao, Appl. Phys. Lett. **82**, 4823 (2003).
[10] F. Quéré, S. Guizard, and P. Martin, Europhys. Lett. **56**, 138 (2001).
[11] B. Rethfeld, Phys. Rev. Lett. **92**, 187401 (2004).
[12] M. Garcia and K. Jeschke, Appl. Surf. Sci. **61**, 2008 (2003).
[13] S. Mao, F. Quere, S. Guizard, R. Russo, G. Petite, and P. Martin, Appl. Phys. A: Mater. Sci. Process. **A79**, 1695 (2004).
[14] F. Korte, J. Serbin, J. Koch, A. Egbert, C. Fallnich, A. Ostendorf, and B. N. Chichkov, Appl. Phys. A: Mater. Sci. Process. **A77**, 229 (2003).
[15] S. J. Henley, G. M. Fuge, and M. N. R. Ashfold, J. Appl. Phys. **97**, 023304 (2005).
[16] F. Claeyssens, M. N. R. Ashfold, E. Sofoulakis, C. G. Ristoscu, D. Anglos, and C. Fotakis, J. Appl. Phys. **91**, 6162 (2002).
[17] F. Beinhorn, J. Ihlemann, K. Luther, and J. Troe, Appl. Phys. A: Mater. Sci. Process. **A79**, 869 (2004).
[18] M. Okoshi and N. Inoue, Appl. Phys. A: Mater. Sci. Process. **A79**, 841 (2004).
[19] T. Makimura, S. Mitani, Y. Kenmotsum, K. Murakami, M. Mori, and K. Kondo, Appl. Phys. Lett. **85**, 1274 (2004).
[20] L. Juha, M. Bittner, D. Chvostova, *et al.*, Appl. Phys. Lett. **86**, 034109 (2005).
[21] K. Sugioka, S. Wada, H. Tashiro, K. Toyoda, Y. Ohnuma, and A. Nakamura, Appl. Phys. Lett. **67**, 2789 (1995).
[22] D. M. Simanovskii, H. A. Schwettman, H. Lee, and A. J. Welch, Phys. Rev. Lett. **91**, 107601 (2003).
[23] C. W. Carr, H. B. Radousky, and S. G. Demos, Phys. Rev. Lett. **91**, 127402 (2003).
[24] K. Rubahn, J. Ihlemann, G. Jakopic, A. C. Simonsen, and H. G. Rubahn, Appl. Phys. A: Mater. Sci. Process. **A79**, 1715 (2004).
[25] L. Sudrie, A. Couairon, M. Franco, B. Lamouroux, B. Prade, S. Tzortzakis, and A. Mysyrowicz, Phys. Rev. Lett. **89**, 186601 (2002); A. Couairon, L. Sudrie, M. Franco, B. Prade, and A. Mysyrowicz, Phys. Rev. B **71**, 125435 (2005).
[26] A. Kaiser, B. Rethfeld, M. Vicanek, and G. Simon, Phys. Rev. B **61**, 11437 (2000).
[27] T. Q. Jia, X. X. Li, D. H. Feng, C. F. Cheng, R. X. Li, H. Cheng, and Z. Z. Xu, Appl. Phys. A: Mater. Sci. Process. **A81**, 645 (2005).
[28] T. Q. Jia, Z. Z. Xu, R. X. Li, D. H. Feng, X. X. Li, C. F. Cheng, H. Y. Sun, N. S. Xu, and H. Z. Wang, J. Appl. Phys. **95**, 5166 (2004).
[29] D. Arnold and E. Cartier, Phys. Rev. B **46**, 15102 (1992).
[30] S. C. Jones, P. Braunlich, R. T. Casper, X. A. Shen, and P. Kelly, Opt. Eng. **28**, 1039 (1989).
[31] H. X. Chen, T. Q. Jia, M. Huang, F. L. Zhao, H. Kuroda, and Z. Z. Xu, Jpn. J. Appl. Phys., Part 1 **45**, 28 (2006).
[32] A. Yakar and B. Byer, J. Appl. Phys. **96**, 5316 (2004).
[33] X. X. Li, T. Q. Jia, D. H. Feng, and Z. Z. Xu, Appl. Surf. Sci. **225**, 339 (2004).
[34] D. Ashkenasi, H. Varel, A. Rosenfeld, F. Noack, and E. E. B. Campbell, Appl. Phys. A: Mater. Sci. Process. **A63**, 103 (1996).
[35] A. Borowiec and H. K. Haugen, Appl. Phys. A: Mater. Sci. Process. **A79**, 521 (2004).
[36] D. C. Deshpande, A. P. Malshe, E. A. Stach, V. Radmilovic, D. Alexander, D. Doerr, and D. Hirt, J. Appl. Phys. **97**, 074316 (2005).
[37] H. O. Jeschke, M. E. Garcia, M. Lenzner, J. Bonse, J. Kruger, and W. Kautek, Appl. Surf. Sci. **197-198**, 839 (2002).
[38] J. M. Liu, Opt. Lett. **7**, 196 (1982).
[39] P. Audebert, P. Daguzan, A. Do Santos, J. C. Gauthier, J. P. Geindre, S. Guizard, G. Hamoniaux, K. Krastev, P. Martin, G. Petite, and A. Antonetti, Phys. Rev. Lett. **73**, 1990 (1994); P. Martin, S. Guizard, P. Daguzan, G. Petite, P. Doliveira, P. Meynadier, and M. Perdrix, Phys. Rev. B **55**, 5799 (1997).
[40] M. Li, S. Menon, J. P. Nibarger, and G. N. Gibson, Phys. Rev. Lett. **82**, 2394 (1999).
[41] J. P. Callan, A. M.-T. Kim, C. A. D. Roeser, and E. Mazur, Phys. Rev. B **64**, 073201 (2001).
[42] S. Guizard, P. Martin, Ph. Daguzan, G. Petite, P. Audebert, J. P. Geindre, A. Dos Santos, and A. Antonnetti, Europhys. Lett. **29**, 401 (1995).
[43] F. Quéré, S. Guizard, P. Martin, G. Petite, O. Gobert, P. Meynadier, and M. Perdrix, Appl. Phys. B: Lasers Opt. **B68**, 459 (1999).
[44] X. Mao, S. S. Mao, and R. E. Russo, Appl. Phys. Lett. **82**, 697 (2003).
[45] A. Flousse, C. Rischel, S. Fourmaux *et al.*, Nature (London) **410**, 65 (2001).
[46] K. Sokolowski-Tinten, C. Blome, C. Dietrich, A. Tarasevitch, M. Horn von Hoegen, D. von der Linde, A. Cavalleri, J. Squier, and M. Kammler, Phys. Rev. Lett. **87**, 225701 (2001).
[47] A. Cavalleri, H. H. W. Chong, S. Fourmaux, T. E. Glover, P. A. Heimann, J. C. Kieffer, B. S. Mun, H. A. Padmore, and R. W. Schoenlein, Phys. Rev. B **69**, 153106 (2004).
[48] Q. Sun, H. Jiang, Y. Liu, Z. Wu, H. Yang, and Q. Gong, Opt. Lett. **30**, 320 (2005).
[49] R. Lindner, M. Reichling, R. T. Williams, and E. Matthias, J. Phys.: Condens. Matter **13**, 2339 (2001).
[50] T. Tsujibayashi, M. Watanabe, O. Arimoto, M. Itoh, S. Nakanishi, H. Itoh, S. Asaka, and M. Kamada, Phys. Rev. B **60**, R8442 (1999).
[51] R. Lindner, R. T. Williams, and M. Reichling, Phys. Rev. B **63**, 075110 (2001).
[52] B. K. Ridly, *Quantum Processes in Semiconductors* (Clarendon, Oxford, 1988).
[53] T. Q. Jia, R. X. Li, Z. Liu, H. Chen, and Z. Z. Xu, Appl. Surf. Sci. **189**, 78 (2002).
[54] A. H. Kahn, Phys. Rev. **97**, 1647 (1955).
[55] W. Kaiser, R. J. Collins, and H. Y. Fan, Phys. Rev. **91**, 1380 (1953).
[56] W. Spitzer and H. Y. Fan, Phys. Rev. **108**, 268 (1957).

[57] D. E. Aspnes, E. Kinsbron, and D. D. Bacon, Phys. Rev. B **21**, 3290 (1980).
[58] L. X. Benedict, J. E. Klepeis, and F. H. Streitz, Phys. Rev. B **71**, 064103 (2005).
[59] E. D. Palik, *Handbook of Optical Constants of Solids* (Academic Press, New York, 1985).
[60] A. Horn, H. Khajehnouri, E. Kreutz, and R. Poprawe, Proc. SPIE **4948**, 393 (2003).
[61] K. Tanimura, Phys. Rev. B **63**, 184303 (2001).
[62] E. Gnani, S. Reggiani, and M. Rudan, Phys. Rev. B **66**, 195205 (2002).
[63] J. R. Chelikowsky and M. Schülter, Phys. Rev. B **15**, 4020 (1977).
[64] A. Belsky, P. Martin, H. Bachau, A. N. Vasil'ev, B. N. Yatsenko, S. Guizard, G. Geoffroy, and G. Petite, Europhys. Lett. **67**, 301 (2004).
[65] L. V. Keldysh, Sov. Phys. JETP **20**, 1307 (1965).
[66] G. W. C. Kaye and T. H. Laby, *Tables of Physical and Chemical Constants* (Longman, New York, 1986).
[67] K. Sokolowski-Tinten and D. vonder Linde, Phys. Rev. B **61**, 2643 (2000).
[68] G. T. Kiehne, A. E. Kryukov, and J. B. Ketterson, Appl. Phys. Lett. **75**, 1676 (1999).
[69] T. Jia, H. Chen, H. Q. Li, R. X. Li, and Z. Z. Xu, Phys. Rev. A **64**, 043811 (2001).
[70] A. V. Balakin, V. A. Bushuev, N. I. Koroteev, B. I. Mantsyzov, I. A. Ozheredov, and A. Shkurinov, Opt. Lett. **24**, 793 (1999).
[71] Ch. Ziener, P. S. Foster, E. J. Divall, C. J. Hooker, M. H. R. Hutchinson, A. J. Langley, and D. Neely, J. Appl. Phys. **93**, 768 (2003).